

**Monitoring the effect
of upwelling on the
chlorophyll *a* distribution
in the Gulf of Finland
(Baltic Sea) using remote
sensing and in situ data***

doi:10.5697/oc.54-3.395
OCEANOLOGIA, 54 (3), 2012.
pp. 395–419.

© Copyright by
*Polish Academy of Sciences,
Institute of Oceanology,
2012.*

KEYWORDS
MERIS
MODIS
Upwelling
Chlorophyll *a*
SST
Baltic Sea
Gulf of Finland

RIVO UIBOUPIN*
JAAN LAANEMETS
LIIS SIPELGAS
LAURA RAAG
INGA LIPS
NATALIA BUHHALKO

Marine Systems Institute,
Tallinn University of Technology,
Akadeemia 15a, Tallinn 12618, Estonia;

e-mail: rivo.uiboupin@msi.ttu.ee

*corresponding author

Received 12 March 2012, revised 17 April 2012, accepted 8 May 2012.

Abstract

The spatio-temporal variability of chlorophyll *a* (Chl *a*) caused by a sequence of upwelling events in the Gulf of Finland in July–August 2006 was studied using remote sensing data and field measurements. Spatial distributions of sea surface temperature (SST) and Chl *a* concentration were examined using MODIS and MERIS data respectively. The MERIS data were processed with an algorithm

* The study was supported by the Estonian Science Foundation (grants No. 7467, No. 6752, No. 7633, No. 7581 & No. 8968). The remote sensing data were provided by ESA via Cat-1 project No. 6855.

The complete text of the paper is available at <http://www.iopan.gda.pl/oceanologia/>

developed by the Free University of Berlin (FUB) for case 2 waters. Evaluation of MERIS Chl *a* versus in situ Chl *a* showed good correlation ($r^2 = 0.67$), but the concentration was underestimated. The linear regression for a 2 h window was applied to calibrate MERIS Chl *a*. The spatio-temporal variability exhibited the clear influence of upwelling events and related filaments on Chl *a* distribution in the western and central Gulf. The lowest Chl *a* concentrations were recorded in the upwelled water, especially at the upwelling centres, and the highest concentrations (13 mg m^{-3}) were observed about two weeks after the upwelling peak along the northern coast. The areas along the northern coast of upwelled water (4879 km^2) on the SST map, and increased Chl *a* (5526 km^2) two weeks later, were roughly coincident. The effect of upwelling events was weak in the eastern part of the Gulf, where Chl *a* concentration was relatively consistent throughout this period.

1. Introduction

Remote sensing data have been widely used for monitoring the ecological and physical state of the Baltic Sea. Satellite imagery has been used for detecting interannual, seasonal and mesoscale variability of the sea surface temperature (SST) (Horstmann 1983, Gidhagen et al. 1987, Siegel et al. 1994, Krężel et al. 2005a, Siegel et al. 2006, Bradtke et al. 2010). Previous studies have demonstrated that remote sensing imagery can be used for the systematic monitoring of the chlorophyll *a* (Chl *a*) distribution and variability (Krężel et al. 2005b, Koponen et al. 2007, Kratzer et al. 2008). Coastal upwelling is an important process that brings cold, nutrient-rich deep water to the surface layer, and can be monitored using different remote sensing data (Krężel et al. 2005a, Lass et al. 2010). The combined use of SST and Chl *a* imagery, complemented by in situ measurements and wind information, provides a basis for describing and analysing the spatial variability of phytoplankton blooms promoted by upwelling.

The Gulf of Finland is an area of the Baltic Sea well known for frequent upwelling events (Kahru et al. 1995, Myrberg & Andrejev 2003, Lehmann & Myrberg 2008, Myrberg et al. 2008). Satellite SST data have shown that during the strongest upwelling events along the northern and southern coasts of the Gulf of Finland, the upwelled water can cover remarkably large areas, corresponding to about 40% and 20%, respectively, of the total surface area of the Gulf (which is about $29\,500 \text{ km}^2$) (Uiboupin & Laanemets 2009). During upwelling events the surface phytoplankton community is transported offshore and replaced by species normally resident in the upper part of the thermocline (Kanoshina et al. 2003, Vahtera et al. 2005, Lips & Lips 2010). Numerical simulations by Zhurbas et al. (2008) and field measurements by Lips et al. (2009) have shown that in the narrow, elongated Gulf of Finland, upwelling along one coast is accompanied by downwelling along the opposite coast, i.e. two longshore baroclinic jets and

their related thermohaline fronts develop simultaneously. The instability of a longshore baroclinic jet leads to the increasing development of filaments and eddies, and thus coastal offshore mixing, resulting in a substantial horizontal variability of the surface layer temperature, upwelled nutrients and phytoplankton/chlorophyll.

The spatio-temporal variability of hydrographic and biological-chemical parameters can be regularly monitored from autonomous ship-of-opportunity measurements that collect temperature, salinity and chlorophyll *a* fluorescence data, as well as water samples for nutrient and phytoplankton analysis, along fixed transects in the Baltic Sea (Rantajärvi et al. 1998, Lips & Lips 2008, Petersen et al. 2008). However, for obtaining information about the phytoplankton abundance/biomass, and surface distribution over large sea areas, remote sensing imagery is invaluable. The Baltic Sea (including the Gulf of Finland) comprises optically complex case 2 waters that are dominated by coloured dissolved organic matter, and it is therefore a considerable challenge to produce accurate estimates of water quality parameters from remote sensing imagery (Schroeder et al. 2007a, Sorensen et al. 2007, Kratzer et al. 2008). This optical complexity affects satellite Chl *a* retrievals, so it is important to validate the algorithm using in situ measurements. Satellite imagery with sufficient temporal resolution is regularly available from MERIS (Medium Resolution Imaging Spectrometer) and MODIS (Moderate Resolution Imaging Spectroradiometer) for the Baltic Sea region. MERIS was designed to monitor coastal waters (Doerffer et al. 1999), and it therefore has sufficient spectral resolution in the visible range to monitor turbid waters like the Baltic Sea. In principle, MERIS operates in a range enabling the detection of pigments like phycocyanin (cyanobacteria), which have specific absorption minima near wavelength 630 nm and local maxima at wavelength 650 nm (Kutser et al. 2006).

A series of upwelling events along the northern and southern coasts of the Gulf of Finland occurred in July–August 2006. Westerly winds were dominant in July, generating moderate upwelling along the northern coast of the Gulf. Easterly winds then prevailed during the whole of August, and as a result, very intense upwelling was observed along the southern coast. The upwelling events were well documented by several studies based on in situ measurements of physical, biological and chemical parameters (Suursaar & Aps 2007, Lips et al. 2009, Lips & Lips 2010). In addition, remote sensing data (MERIS and MODIS) are available from that period to monitor the variability of SST and phytoplankton chlorophyll *a* fields.

The objectives of this study were: (1) to validate the MERIS chlorophyll product retrieved with the Free University of Berlin (FUB) case 2 waters processor using in situ measurements of Chl *a*, and (2) to assess the spatial

and temporal variability of the Chl *a* field caused by consecutive upwelling events using MERIS data.

This paper is structured as follows: section 2 describes the in situ, remote sensing and wind data, as well as the methodology; in section 3, the comparability of in situ and satellite chlorophyll *a* data is evaluated, the sequence of upwelling events is described on the basis of MODIS SST, MERIS chlorophyll is compared with in situ chlorophyll *a*, and the upwelling-related variability of the chlorophyll *a* field from MERIS data is described; section 4 discusses the results of the SST and chlorophyll *a* surface distributions; the final conclusions are drawn in section 5.

2. Data and methodology

2.1. In situ data

The in situ data were obtained during five surveys (Table 1) conducted along the same transect between Tallinn and Helsinki (Kuvaldina et al. 2010). Water samples for phytoplankton and Chl *a* analysis were collected from 14 stations, each about 5.2 km apart (Figure 1). Three (but two in the case of the shallow upper mixed layer) water samples were taken from the upper mixed layer (UML, from a depth of 1 m down to the seasonal thermocline) to form a pooled sample for each station. The depth of the UML was determined from the CTD profile, which preceded water sampling. Chl *a* content was measured spectrophotometrically (Thermo Helios γ ; photometric accuracy: ± 0.005 A at 1 A) from the pooled samples in the laboratory (HELCOM 1988). On 19–20 July, two (TH19, TH21) out of five pooled samples were cloud-free on the satellite imagery. Because of inclement weather conditions, only surface samples ($n = 8$) were collected at stations TH1–TH15.

Phytoplankton species composition and biomass were analysed for each survey from pooled samples (Lips & Lips 2010).

Table 1. In situ sampling and MERIS acquisition dates, times (UTC) and number of samples used (N) in July–August 2006. The figures in brackets indicate the number of samples collected within the 2 h interval from the satellite overpass. On 19–20 July, 2 pooled samples and 8 surface samples were collected

Sampling date	N	MERIS date	MERIS time
11 Jul.	14 (3)	11 Jul.	9.35
19–20 Jul.	10	18 Jul.	9.15
25 Jul.	14 (4)	25 Jul.	8.55
8 Aug.	12	7 Aug.	8.46
15–16 Aug.	9	16 Aug.	9.03

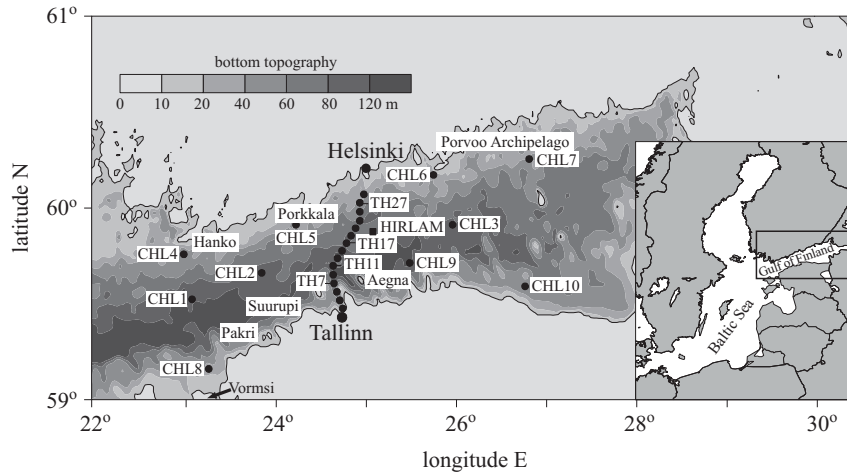


Figure 1. Map of the study area in the Gulf of Finland. The solid circles (●) represent the locations of the in situ sampling stations (TH1–TH27) and the locations of the MERIS chlorophyll time series (CHL1–CHL10, TH7 and TH27). The solid square (■) represents the location of the HIRLAM grid point where wind data were extracted. The bottom topography is drawn from the gridded topography in metres (Seifert et al. 2001)

2.2. MERIS data

MERIS reduced-resolution (about 1×1 km) images from 10 July to 18 August 2006 (altogether 31 sufficiently cloud free images) were used to analyse the spatio-temporal variability of the Chl *a* field. The MERIS images were processed using an algorithm developed by FUB for case 2 waters (Schroeder et al. 2007a, b) to apply an atmospheric correction and to obtain the reflectance values used to calculate the Chl *a* concentration. For the purposes of comparison, we also calculated Chl *a* and reflectance values using the case 2 regional water (C2RW) processor (Doerffer & Schiller 2007).

To compare the MERIS and in situ Chl *a* data, two time frames were selected at 24 h and 2 h intervals (before, or after) from the satellite overpass (Table 1). According to Kratzer et al. (2008) a 2 h window is sufficient for validating satellite Chl *a* measurements with in situ data. The MERIS image pixel covering the location of the sampling station within the given time window was extracted.

To evaluate the suitability of MERIS data for the detection of moderate concentrations of cyanobacteria, the normalized reflectance spectra were calculated according to Wu (2004).

For the detection of surface phytoplankton accumulations a Maximum Chlorophyll Index (MCI) was calculated for each MERIS image using the algorithm provided in Gower et al. (2008).

2.3. MODIS data

To determine the extent of the upwelling zone and to describe the temporal course of SST at selected locations, MODIS data (standard level 2 MODIS SST products) from 10 July to 18 August 2006 were used (<http://oceancolor.gsfc.nasa.gov>). Altogether 200 MODIS/Terra and MODIS/Aqua images (1×1 km pixel spacing) were examined in order to extract the SST data from 60 images that were sufficiently cloud-free.

2.4. Wind data

Wind-induced mixing largely determines the distribution of phytoplankton in the upper layer. To evaluate the comparability of satellite and in situ Chl *a* measurements, wind data from the version of HIRLAM (High Resolution Limited Area Model) of the Estonian Meteorological and Hydrological Institute (Männik & Merilain 2007) were interpolated to the location ($25^{\circ}7.5'E$, $59^{\circ}51.9'N$) close to the measurement transect in July–August 2006 (Figure 1). The spatial resolution of HIRLAM is 11 km, and the forecast interval of 1 h ahead of 54 h is recalculated after every 6 h. To characterize wind-induced mixing we used the depth of the turbulent Ekman boundary layer estimated by the formula $h = 0.1u_*/f$ (Csanady 1982), where $u_* = (\tau/\rho_w)^{1/2}$ is the friction velocity, $\tau = \rho_a C_a u^2$ is the wind stress, $\rho_a = 1.3 \text{ kg m}^{-3}$ is the air density, $C_a = 1.2 \times 10^{-3}$ is the dimensionless wind drag coefficient, u is the wind speed, $\rho_w = 1005 \text{ kg m}^{-3}$ is the water density, and $f = 1.25 \times 10^{-4} \text{ s}^{-1}$ is the Coriolis parameter.

3. Results

3.1. Comparability of in situ and satellite Chl *a*

Generally speaking, remote sensing imagery represents the situation at the sea surface. Variable wind conditions prevailed during July and August, whilst wind speeds were mainly moderate but with some gusts over 10 m s^{-1} (Figure 2b). In this study, the pooled sample represents the UML, and therefore we suggest that these two datasets are comparable if the depth of the turbulent Ekman boundary layer largely persists during the time interval between the acquisition of the MERIS image and the collection of the water samples. The average UML depths estimated from the CTD profiles within

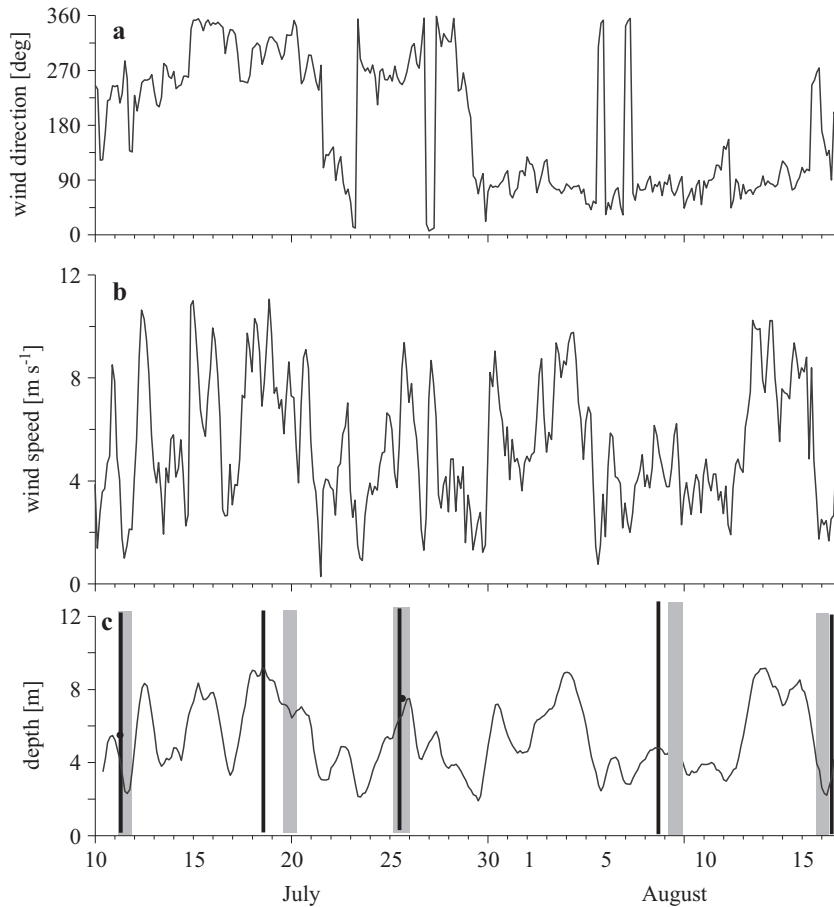


Figure 2. Wind direction (a), wind speed derived from HIRLAM data in July–August 2006 (b), depth of turbulent Ekman boundary layer (c). The grey rectangles mark the time of in situ measurements and the bold lines mark the times of MERIS image acquisition. The black dots represent the UML depths estimated from CTD measurements during the 2 h window on 11 and 25 July

the 2 h windows on 11 July (5.5 m) and 25 July (7.5 m) coincided well with the UML depths estimated from HIRLAM wind data (Figure 2c).

Comparability of in situ and MERIS Chl *a* data is also supported by the MCI calculated from all the MERIS data used. The MCI showed that no surface algal accumulations were observed during the study period. The highest MCI values were observed on 6 August 2006, when a maximum MCI value of $0.9 \text{ mW}/(\text{m}^2 \text{ sr nm})$ was recorded at the location of a filament at the entrance to the Gulf of Finland. The MCI index was close to zero most of the time.

3.2. Upwelling events in July–August

Westerly winds dominated in the Gulf area from 10 to 29 July (Figure 2a). The development of upwelling along the northern coast of the Gulf was observed from 10 July (Figures 3 and 5a), and the temperature difference between the upwelling and the surrounding water was around 5°C for most of the time, according to the MODIS SST data. However, the temperature difference was larger for the upwelling centres because of the

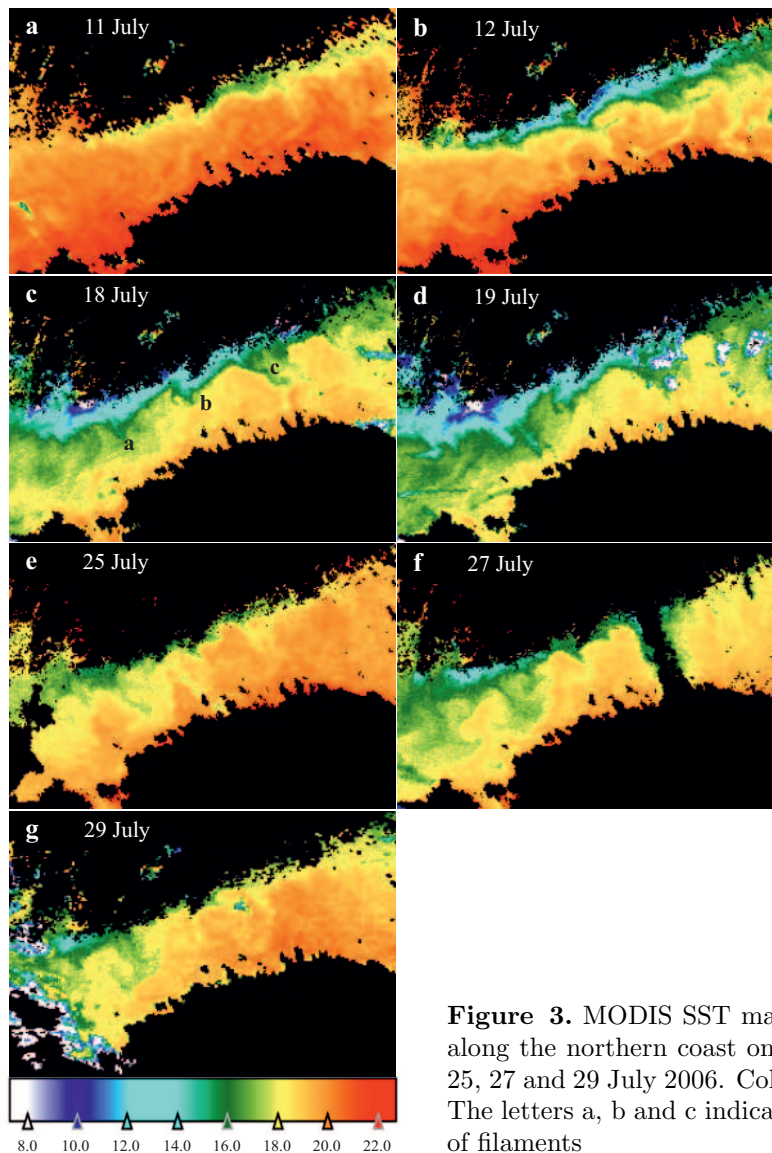


Figure 3. MODIS SST maps of upwelling along the northern coast on 11, 12, 18, 19, 25, 27 and 29 July 2006. Colour scale in °C. The letters a, b and c indicate the locations of filaments

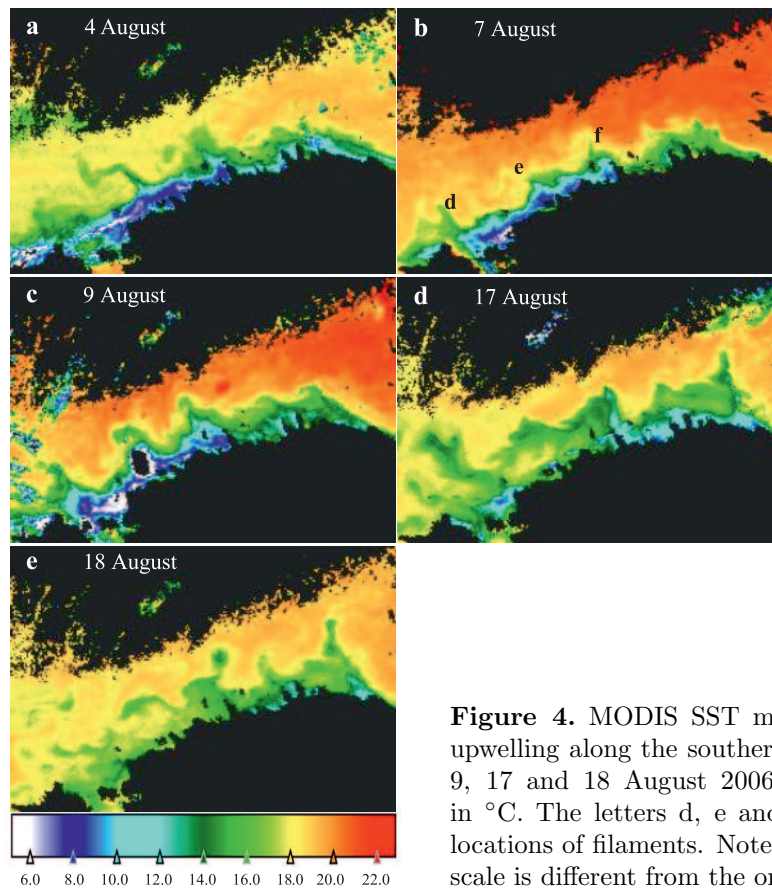


Figure 4. MODIS SST maps of stronger upwelling along the southern coast on 4, 7, 9, 17 and 18 August 2006. Colour scale in °C. The letters d, e and f indicate the locations of filaments. Note that the colour scale is different from the one in Figure 3

significantly lower temperature in the upwelled water. On 12 July the water temperature in the upwelling centre near the Porkkala Peninsula dropped to 8°C (Figure 3b). At the peak of upwelling on 19 July, the upwelling centre was near the Hanko Peninsula (due to the NW wind), and the temperature dropped to 6°C (Figures 3d and 5a), whilst in the middle of the Gulf the temperature was around 16°C, and near the southern coast it was over 18°C (Figure 3d). In the Porkkala region, where the upwelling centre was located on 12 July, the temperature rose to 13°C by 19 July. Relaxation of upwelling along the northern coast started after 20 August as a result of a change in wind forcing (Figure 2). The temperature in the upwelling zone on 25 and 27 July was then in the 14–16°C range, and the surrounding area had temperatures of around 19°C (Figures 3e and f). Because of the start of the upwelling relaxation after 20 July, cold filaments developed off the Hanko and Porkkala Peninsulas, and off the Porvoo Archipelago during the upwelling along the northern coast (Figure 3c).

After 29 July, easterly winds were dominant in the Gulf of Finland area until 16 August (Figure 2a), and as a result, a zone of upwelling formed along the southern coast (Figure 4). The strongest such zone developed along the NW coast of Estonia, from Vormsi Island to Aegna Island, with several upwelling centres near the Pakri Islands, Vormsi Island and off the coast of the Suurupi Peninsula, where the minimum temperature of the upwelled water was about 2°C (Figure 4 and 5b). The temperature difference between the upwelled and the surrounding water was as much as 18°C (Figures 4 and 5b), and the upwelled water covered 31% of the western Gulf area

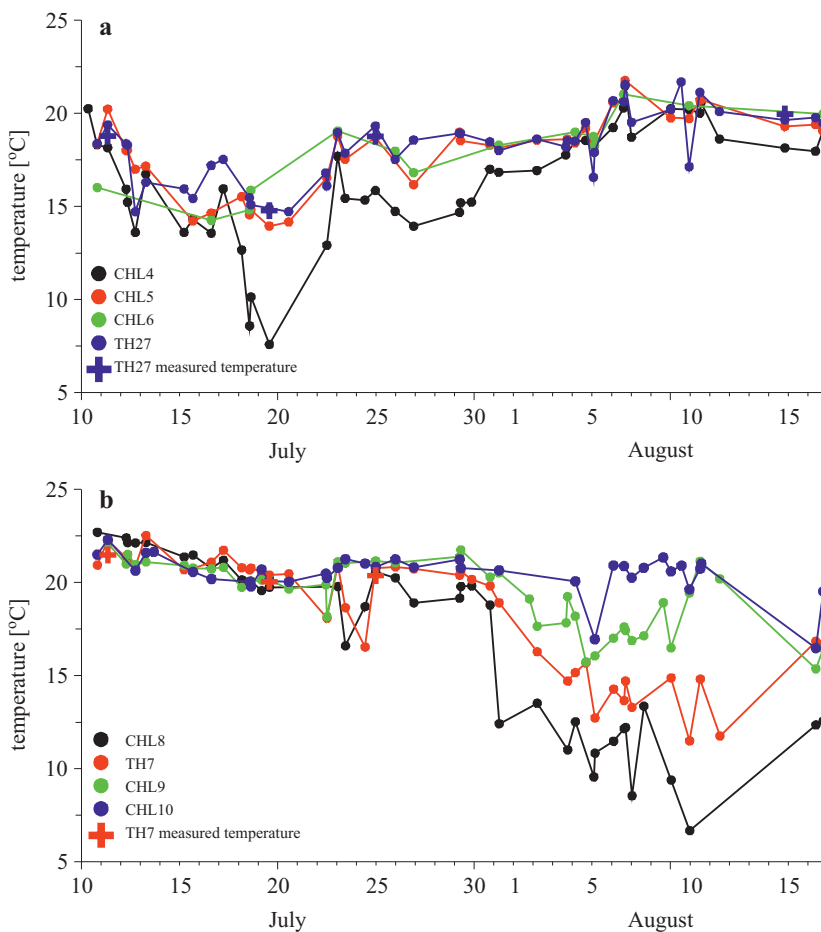


Figure 5. Temporal courses of surface layer temperature (MODIS SST) from 10 July to 16 August 2006 at stations CHL4, CHL5, CHL6 and TH27 (northern part of the Gulf) (a) and at stations CHL8, CHL9, CHL10 and TH7 (southern part of the Gulf) (b). The in situ surface temperature (bold cross) is given for stations TH7 and TH27

(22–26°E) on 9 August. After 16 August, the wind turned to the S and SW (data not shown), thus causing the upwelling to relax. Several cold upwelling filaments developed along the southern coast between longitudes 23 and 27°E, and a few of them transformed into eddies (Figure 4). The filaments were persistent at three locations: north of Hiiumaa, and off Pakri and Tallinn (Figure 4b).

3.3. Evaluation of the FUB Chl *a* processor using in situ Chl *a*

In situ Chl *a* concentrations along the transect varied in a wide range from 1.57 to 15.54 mg m⁻³ during the period of field measurements (Figure 6). Low Chl *a* values were observed during the first half of July in the upwelling region along the northern coast. From 25 July, when upwelling along the northern coast was in the relaxation phase, the Chl *a* concentrations increased off the northern coast, and decreased off the southern coast. The highest (15.5 mg m⁻³) and lowest (1.6 mg m⁻³) Chl *a* concentrations were observed on 8 August off the northern and southern coasts respectively.

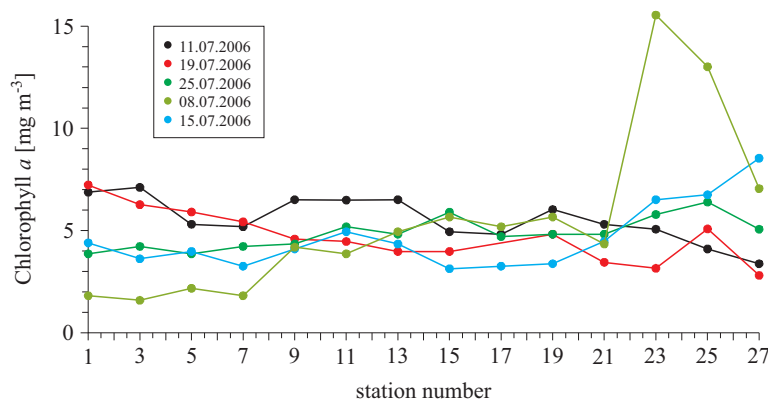


Figure 6. In situ Chl *a* distribution along the sampling transect on 11, 19 and 25 July, and 8 and 15 August 2006

The Chl *a* concentrations calculated with the FUB processor from the MERIS data was correlated with in situ Chl *a* for two time windows: 24 h and 2 h intervals (before or after) from the satellite overpass. A scatterplot of selected data pairs is shown in Figure 7. A total of 7 data pairs fulfilled the 2 h criterion: 3 samples (TH9, TH11 and TH13) from 11 July and 4 samples (TH11, TH13, TH15 and TH17) from 25 July (Table 1). For the 2 h window the FUB processor underestimated Chl *a* compared with in situ Chl *a* (Figure 7); the average underestimation was 25% (1.3 mg m⁻³),

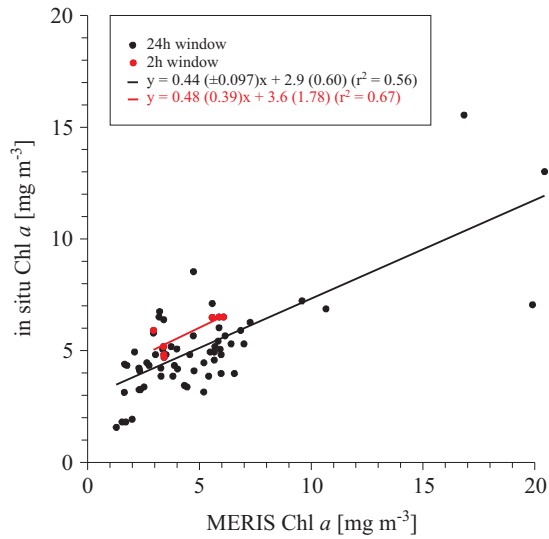


Figure 7. Scatterplot of in situ Chl *a* and MERIS Chl *a* derived by the FUB processor. Black dots represent all data pairs from 11, 18 and 25 July, and 7 and 16 August 2006 (24 h window), and red dots represent data pairs from 11 and 25 July 2006 (2 h window). The data corresponding to the 2 h window were used to estimate bias and to calibrate the FUB Chl *a* processor. The correlation (r^2) for 24 h window data points was 0.56 and for the 2 h window it was 0.67

which is of the same magnitude as in previous studies in the Baltic Sea (Kratzer et al. 2008). The correlation (r^2) for data points within the 2 h window was 0.67 and for the 24 h window was also relatively high at 0.56. The linear regression for the 2 h window with 95% confidence limits was $\text{Chl } a = 0.48(\pm 0.39) \times X + 3.6(\pm 1.8)$, where X is the FUB processor output. The standard deviation of the residuals (i.e. standard error of the estimation – SEE) was 0.51. For the 24 h window the slope and y-intercept of the linear regression were 0.44 (± 0.097) and 2.9 (± 0.60) respectively. The standard deviation of the residuals for the 24 h window was 1.43.

In addition to the FUB processor we also evaluated the case 2 regional water processor (C2RW) for Chl *a* (data not shown). The correlation for the FUB processor (0.67) was much higher compared to the C2RW processor (0.17). Also, the Chl *a* overestimation of C2RW by 52% is poorer compared with the underestimation (25%) by the FUB processor.

On the basis of the above analysis, the FUB algorithm was used to calculate Chl *a* from MERIS data in the Gulf of Finland. The equation obtained with linear regression for the 2 h window was applied to calibrate MERIS Chl *a* data.

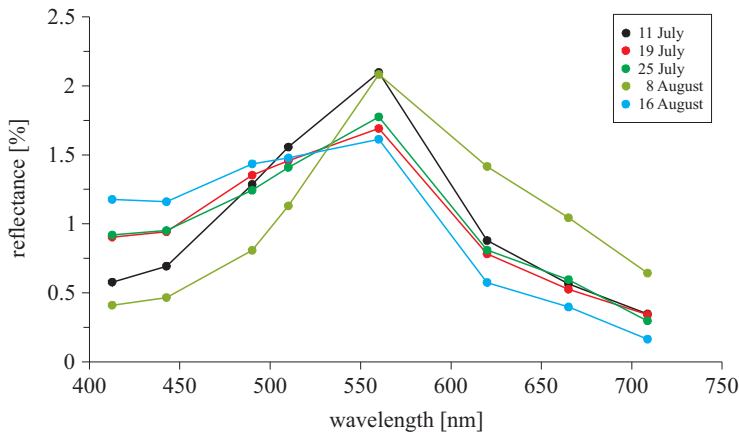


Figure 8. Normalized reflectance spectra calculated according to Wu (2004) on 11, 19 and 26 July; 8 and 16 August 2006 at location TH25

In order to assess the suitability of MERIS data (processed with the FUB algorithm) for detecting cyanobacteria, we analysed the temporal changes of reflectance spectra at the location of the largest increase in Chl *a* off the northern coast (Figure 6). We used MERIS images with the smallest time displacement from the time of the in situ measurements (Table 1). The distinct peak around wavelengths 620–650 nm, which is related to phycocyanin, was not detected on any of the normalized spectra (Figure 8).

3.4. Upwelling-related Chl *a* variability from MERIS imagery

To describe the spatio-temporal variability of the Chl *a* field, we used maps (Figures 9 and 10) and time series (Figure 11) at selected locations (Figure 1) formed from calibrated MERIS Chl *a* data. Different locations were selected to describe the temporal variability of Chl *a* along the northern and southern coasts, and along the axis of the Gulf (open sea area).

In July–August the Chl *a* concentrations were generally higher along the northern coast compared with those in the open sea area, and along the southern coast (Figure 11). In July the Chl *a* concentrations along the northern coast varied in the range of 4–9 mg m⁻³ (Figure 11a). After the relaxation of upwelling along the northern coast, Chl *a* concentrations reached high values of up to 13–14 mg m⁻³ at locations CHL5 and TH27 on 7 August. The increase in Chl *a* was also observed at other locations along the northern coast, reaching values of up to 8.5 mg m⁻³. Elevated Chl *a* along the northern coast and in the filaments was observed starting from 23 July and peaked on 6–7 August (Figures 9e, 10b and c). By 6 August, 26% of the area between longitudes 23–27°E was covered by Chl *a*

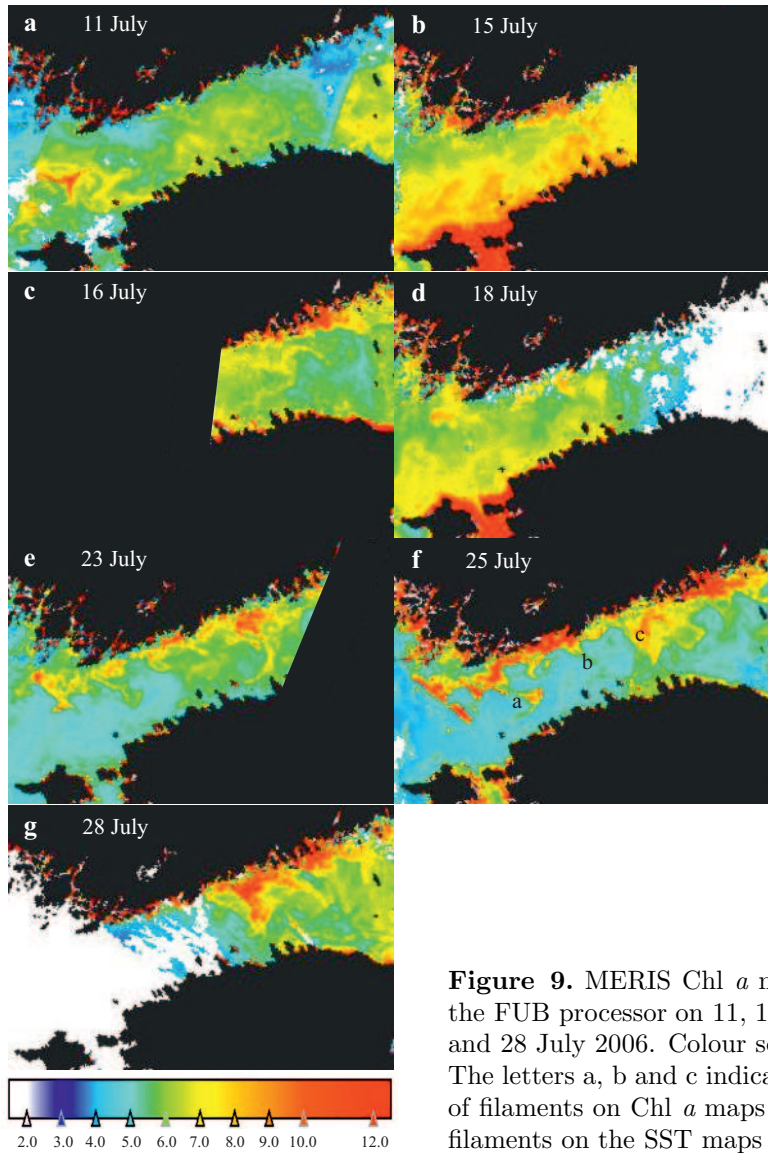


Figure 9. MERIS Chl *a* maps derived by the FUB processor on 11, 15, 16, 18, 23, 25 and 28 July 2006. Colour scale in mg m^{-3} . The letters a, b and c indicate the locations of filaments on Chl *a* maps coincident with filaments on the SST maps (see Figure 3c)

concentrations above 7 mg m^{-3} (Figure 10b and c). The development of the Chl *a* field was characterized by high spatial and temporal variability; standard deviations were 2.1 and 2.4 mg m^{-3} at locations CHL5 and TH27 respectively. Chlorophyll-rich filaments were observed off the Hanko and Porkkala Peninsulas and the Porvoo Archipelago after 23 July, when upwelling along the northern coast was in the relaxation phase. Relatively high and persistent Chl *a* concentrations were observed in the easternmost

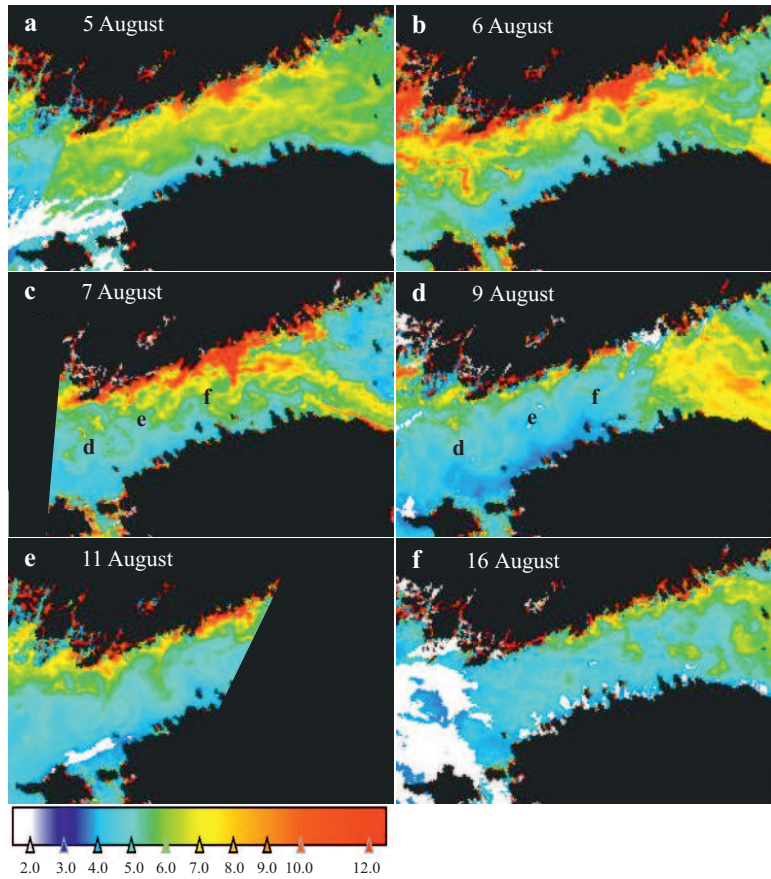


Figure 10. MERIS Chl *a* maps derived by the FUB processor on 5, 6, 7, 9, 11 and 16 August 2006. Colour scale in mg m^{-3} . The letters d, e and f indicate the locations of filaments on Chl *a* maps coincident with filaments on SST maps (see Figures 4b and 4c)

part of the study area (CHL7, mean = 5.9 mg m^{-3} , SD = 1.1 mg m^{-3}) throughout the period.

Along the southern coast, Chl *a* concentrations varied between 4 and 8.5 mg m^{-3} in July–August (Figure 11c). Higher Chl *a* concentrations (up to 8.5 mg m^{-3}) were observed in the western part of the Gulf (CHL8 and TH7) during the upwelling along the northern coast between 11 to 18 July. In early August, when upwelling developed along the southern coast, the temperature dropped below 12°C (Figure 4b), and measured Chl *a* concentrations were below 5 mg m^{-3} (Figure 10c) in a narrow area along the southern coast. The temporal course of Chl *a* along the southern coast was less variable compared with the northern coast during the whole study

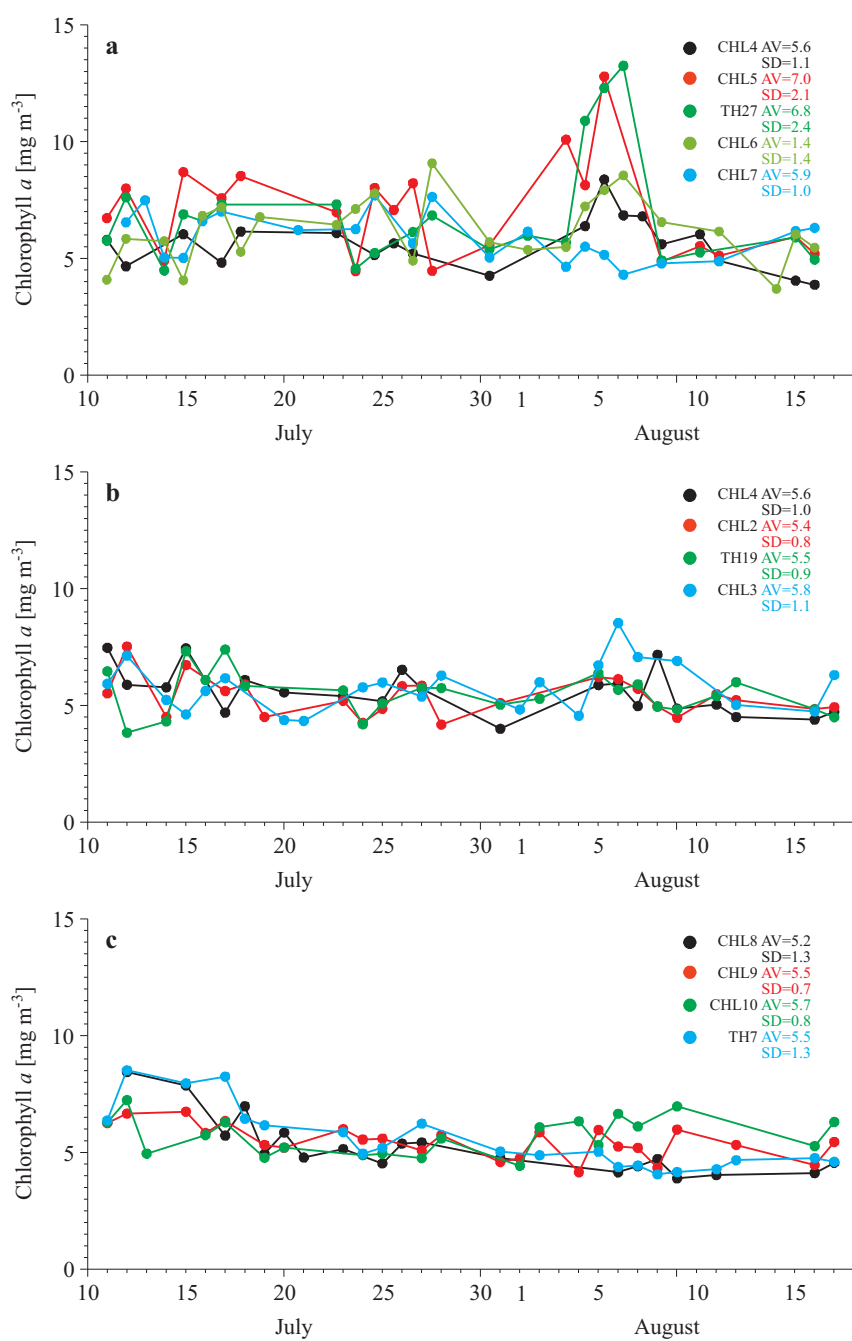


Figure 11. Distribution of MERIS Chl *a* at selected locations (see Figure 1) along the northern coast (a), along the Gulf axis (b), and along the southern coast (c) in July–August 2006

period (Figure 11c). By 16 (and 18) August, when upwelling started to relax (Figure 4e), the Chl *a* concentrations increased slightly in the upwelling region (Figure 9c, CHL8 and TH7). Again, relatively high and persistent Chl *a* concentrations were found in the easternmost part of the study area (CHL10, mean = 5.7 mg m⁻³, SD = 0.8 mg m⁻³).

During the whole study period the temporal course of Chl *a* along the Gulf axis (Figure 11b) displayed less variability, mainly between 4 and 8 mg m⁻³, compared with the northern coast. Chl *a* variations were larger between 11 and 18 July (Figures 9 and 11b), when the upwelling front and related filaments with low chlorophyll contents (Figures 3a–d) reached the open part of the Gulf. The high variability of Chl *a* at locations along the Gulf axis observed in August (Figure 11b, CHL1, CHL2 and TH19) was a result of chlorophyll-rich filaments from the northern, and chlorophyll-poor filaments from the southern, coastal sea areas (Figure 10).

4. Discussion

July–August 2006 was characterized by quite a rare wind regime in the Gulf of Finland: westerly winds prevailed until 29 July, whereas after 30 July easterly winds remained dominant for quite a long time. In the long, narrow Gulf of Finland, westerly winds cause upwelling along the northern coast, and downwelling along the southern coast, and vice versa when winds are blowing from the east. A high-resolution numerical study showed that the instability of the longshore baroclinic jet and related thermohaline fronts, caused by coupled upwelling and downwelling events, leads to the development of cold and warm mesoscale filaments and eddies contributing to coastal offshore exchange (Zhurbas et al. 2008). The maps of mean mesoscale (eddy) kinetic energy in the surface layer (simulation for July–August 2006), showed that the coastal offshore exchange caused by filaments and eddies is larger in the narrow western and the central parts of the Gulf (Laanemets et al. 2011).

Spatio-temporal variability of the Chl *a* field observed from MERIS imagery in July–August 2006 clearly reflected the influence of mesoscale physical processes, coupled upwelling/downwelling events and related filaments. Wind mixing may also decrease the surface Chl *a* concentration by mixing phytoplankton deeper into the water column. Chl *a* concentrations varied in a wide range, from 4 to 14 mg m⁻³, which is also expressed in the variations of mean concentrations (5.2–7.0 mg m⁻³) and standard deviations (SD = 1.4–2.4 mg m⁻³) (Figures 9, 10 and 11). Chl *a* concentrations were the lowest in the upwelling zones along both coasts. The highest mean Chl *a* and standard deviation were recorded along the northern coast: up to 7.0 and 2.4 mg m⁻³ respectively. In this region the upwelling and possible

upwelling-related nutrient input to the surface layer occurred earlier, during the first half of July, and therefore most likely promoted phytoplankton growth after the relaxation of the upwelling and the warming of the surface layer.

At locations along the Gulf axis in the western and central Gulf of Finland, the variability of the surface Chl *a* field (Figure 11b) was related to mesoscale activity. In July, when upwelling was taking place along the northern coast, filaments carried cold water with low chlorophyll concentrations offshore. In August, filaments carried chlorophyll-poor water from the southern upwelling zone and chlorophyll-rich water from the northern downwelling zone, into the central part of the Gulf.

In the shallower eastern part of the Gulf, the mesoscale activity estimated from SST imagery (Kahru et al. 1995, Uiboupin & Laanemets 2009) and numerical simulations (Laanemets et al. 2011) was lower. This was also reflected by the MERIS Chl *a* data, as concentrations were relatively persistent (mean 5.7–5.9 mg m⁻³) with small standard deviations (0.8–1.1 mg m⁻³).

The largest increase in Chl *a* was observed from 4 to 8 August along the northern coast (Figures 11a and 12) after the decrease of the surface Chl *a* concentration from 31 July to 4 August (Figures 11a and b), which was most likely caused by a strong wind event increasing the UML depth (Figures 2b and c) and mixing the phytoplankton deeper. There are probably two reasons for the increase of Chl *a* concentration in the narrow northern coastal zone and the cold filaments (Figure 9e) starting after the peak of upwelling

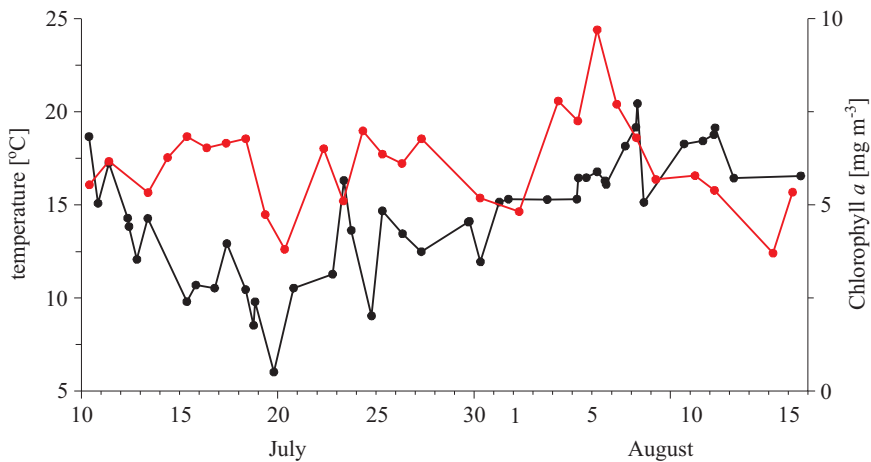


Figure 12. Temporal course of average (CHL4, CHL5 and CHL6) Chl *a* concentration (red line), and SST (black line) on the northern coast in July–August 2006

on 20 July (Figure 12). One reason could be the phytoplankton growth promoted by nutrient input during the upwelling in July along the northern coast. The numerical simulation of nutrient transport during upwelling events in summer 2006 showed that the main area along the northern coast of the Gulf, where nutrients (nitrogen and phosphorus) were brought to the surface layer, was from the Hanko Peninsula to the Porvoo Archipelago region (Laanemets et al. 2011). By 20 July most of the nitrogen and phosphorus (about 325 and 400 tonnes respectively) had been brought into the upper layer (Laanemets et al. 2009). This area coincided with the area of intensive upwelling along the northern coast depicted on the SST maps (Figures 3b and c). After the upwelling began to relax, the temperature in the northern coastal zone rose to above 15°C by 23 July (Figures 5a and 12). Previous studies have shown that phytoplankton growth is promoted in an area covered by upwelled nutrient-rich water (Vahtera et al. 2005). To confirm this assumption, we also compared the upwelled water area and the extended Chl *a* area along the northern coast. The area where the temperature was < 14°C, i.e. the narrow area along the northern coast where nutrients were probably brought to the surface layer, was 1317 km² (about 7% of the study area) on 18 July. Moreover, the area along the coast of water with a temperature < 17°C due to offshore transport and also covering the filaments was 4879 km² (about 25%). The upwelling-induced area with a slightly increased Chl *a* (concentrations over 7 mg m⁻³) on 25 July was 5507 km². This area remained approximately the same until 6 August (the bloom peak) – 5526 km². This suggests that the observed phytoplankton increase occurred mainly in the region of possible nutrient input by upwelling with a two week lag. Of course, some differences in the spatial distribution were due to the development of upwelling along the southern coast (Figures 4a and b).

The second possible reason responsible for the higher Chl *a* concentrations and variability along the northern coast could be the Ekman transport of phytoplankton biomass in the surface layer from the open sea area towards the northern coast during the upwelling event along the southern coast and the simultaneous downwelling along the northern coast in early August. Surface transport and a higher Chl *a* concentration in the downwelling zone were also observed in previous studies (Pavelson et al. 1999, Kanoshina et al. 2003, Lips & Lips 2010). In addition, Lips & Lips (2010) found a relationship between high phytoplankton biomass and a mesoscale anticyclonic feature in the northern part of the study area on 8 August. This corresponds to Zhurbas et al. (2006), who showed that instability of the longshore baroclinic jet, associated with downwelling, results in the formation of an anticyclonic eddy. The highest biomass values in the same area coincided

with this mesoscale feature, where domed isopycnals caused shallowing of the UML to only 5 m, against the background of a relatively deep UML in the remainder of the downwelling area on the transect. The northward surface transport of cold upwelled water and the spreading of filaments with low chlorophyll content are clearly visible on the SST and Chl *a* maps (Figures 4a, b, c and 10a, b, c, d).

The distinct feature (the peak around 630 nm) in the red part of the reflectance spectrum can be used to detect phycocyanin (cyanobacteria) (Dekker 1993, Dekker & Peters 1993, Reinart & Kutser 2006, Kutser et al. 2006). Bio-optical modelling results by Metsamaa et al. (2006) showed that MERIS bands 6 and 7 can be used to separate cyanobacteria and green algae if the concentration of Chl *a* in the cyanobacteria is 8–10 mg m⁻³. The calculated reflectance spectra showed that despite the dominance of phycocyanin-containing cyanobacteria (Chl *a* about 9 mg m⁻³) off the northern coast on 8 August (Lips & Lips 2010), the peak around 630 nm was not detected (Figure 8). Thus, our estimates based on in situ data confirmed the bio-optical modelling result. Previous field measurements have shown that Chl *a* in cyanobacteria during blooms were usually 10 mg m⁻³ in the Gulf of Finland area (Kononen et al. 1996, Vahtera et al. 2005, Suikkanen et al. 2007), i.e. cyanobacteria blooms are not detectable on MERIS imagery before the appearance of surface accumulations.

5. Conclusions

Upwelling events along the northern (southern) coast of the Gulf of Finland led to a minimum temperature of around 6°C (2°C) with a temperature difference between the upwelled and surrounding water of up to 12°C (18°C).

The Chl *a* concentration obtained from MERIS data using the FUB processor was well correlated with in situ measurements ($r^2 = 0.67$), but was underestimated on average by 25%. The Chl *a* concentration in cyanobacteria was not high enough to detect the characteristic feature of phycocyanin around wavelengths 620–650 nm in the reflectance spectra.

The spatio-temporal variability of Chl *a* estimated from MERIS data showed the evident influence of upwelling events and related filaments. The variability of Chl *a* was largest in the western and central parts of the Gulf, where mesoscale activity was the highest.

The highest Chl *a* concentrations (up to 14 mg m³) along the northern coast were observed about two weeks after the upwelling peak. The high Chl *a* was induced by (1) growth of phytoplankton promoted by nutrient input, and (2) the northward Ekman transport of surface waters caused by easterly wind forcing at the beginning of August.

Comparison of the upwelling areas on the SST images and high Chl *a* areas on MERIS images showed structural similarities. The upwelling area along the northern coast (4879 km²) and the high Chl *a* area (5526 km²) about two weeks later were roughly coincident. Also, the filaments with high Chl *a* coincided with the locations of cold filaments extending from the upwelling front along the northern coast. In the case of intensive upwelling along the southern coast, the low Chl *a* regions coincided with the cold filaments.

Upwelling events had only a minor influence in the eastern part of the study area, where Chl *a* concentrations were relatively high and persistent throughout the study period.

Acknowledgements

Our thanks go to the staff of the Marine Systems Institute who conducted the measurement campaigns.

References

- Bradtke K., Herman A., Urbański J. A., 2010, *Spatial and interannual variations of seasonal sea surface temperature patterns in the Baltic Sea*, *Oceanologia*, 52 (3), 345–362, <http://dx.doi.org/10.5697/oc.52-3.345>.
- Csanady G. T., 1982, *Circulation in the coastal ocean*, D. Reidel Publ. Co., Dordrecht, 279 pp.
- Dekker A. G., 1993, *Detection of optical water quality parameters for eutrophic waters by high resolution remote sensing*, Ph.D. thesis, Free University, Amsterdam.
- Dekker A. G., Peters S. W. M., 1993, *The use of the thematic mapper for the analysis of eutrophic lakes – a case-study in the Netherlands*, *Int. J. Remote Sens.*, 14 (5), 799–821, <http://dx.doi.org/10.1080/01431169308904379>.
- Doerffer R., Sorensen K., Aiken J., 1999, *MERIS potential for coastal zone applications*, *Int. J. Remote Sens.*, 20 (9), 1809–1818, <http://dx.doi.org/10.1080/014311699212498>.
- Doerffer R., Schiller H., 2007, *The MERIS case 2 water algorithm*, *Int. J. Remote Sens.*, 28 (3–4), 517–535, <http://dx.doi.org/10.1080/01431160600821127>.
- Gidhagen L., 1987, *Coastal upwelling in the Baltic – satellite and in situ measurements of sea surface temperatures indicating coastal upwelling*, *Estuar. Coast. Shelf Sci.*, 24 (4), 449–462, [http://dx.doi.org/10.1016/0272-7714\(87\)90127-2](http://dx.doi.org/10.1016/0272-7714(87)90127-2).
- Gower J., King S., Borstad G., Brown L., 2008, *The importance of a band at 709 nm for interpreting water-leaving spectral radiance*, *Can. J Remote Sens.*, 34 (3), 287–295.

- HELCOM, 1988, *Guidelines for the Baltic Monitoring Programme for the third stage*, Baltic Sea Environ. Proc., 27D.
- Horstmann U., 1983, *Distribution patterns of temperature and water colour in the Baltic Sea as recorded in satellite images: Indicators for phytoplankton growth*, Ber. Inst. Meeresk., Kiel, 106, 147 pp.
- Kahru M.H., Håkansson B., Rud O., 1995, *Distributions of the sea-surface temperature fronts in the Baltic Sea as derived from satellite imagery*, Cont. Shelf Res., 15 (6), 663–679, [http://dx.doi.org/10.1016/0278-4343\(94\)E0030-P](http://dx.doi.org/10.1016/0278-4343(94)E0030-P).
- Kanoshina I., Lips U., Leppänen J.-M., 2003, *The influence of weather conditions (temperature and wind) on cyanobacterial bloom development in the Gulf of Finland (Baltic Sea)*, Harmful Algae, 2 (1), 29–41, [http://dx.doi.org/10.1016/S1568-9883\(02\)00085-9](http://dx.doi.org/10.1016/S1568-9883(02)00085-9).
- Kononen K., Kuparinen J., Mäkelä K., Laanemets J., Pavelson J., Nömmann S., 1996, *Initiation of cyanobacterial blooms in a frontal region at the entrance to the Gulf of Finland, Baltic Sea*, Limnol. Oceanogr., 41 (1), 98–112.
- Koponen S., Attila J., Pulliainen J., Kallio K., Pyhälähti T., Lindfors A., Rasmus K., Hallikainen M., 2007, *A case study of airborne and satellite remote sensing of a spring bloom event in the Gulf of Finland*, Cont. Shelf Res., 27 (2), 228–244, <http://dx.doi.org/10.1016/j.csr.2006.10.006>.
- Kratzer S., Brockmann C., Moore G., 2008, *Using MERIS full resolution data to monitor coastal waters – A case study from Himmerfjärden, a fjord-like bay in the northwestern Baltic Sea*, Remote Sens. Environ., 112 (5), 2284–2300, <http://dx.doi.org/10.1016/j.rse.2007.10.006>.
- Kreżel A., Ostrowski M., Szymelfenig M., 2005a, *Sea surface temperature distribution during upwelling along the Polish Baltic coast*, Oceanologia, 47 (4), 415–432.
- Kreżel A., Szymanek L., Kozłowski L., Szymelfenig M., 2005b, *Influence of coastal upwelling on chlorophyll a concentration in the surface water along the Polish coast of the Baltic Sea*, Oceanologia, 47 (4), 433–452.
- Kutser T., Metsamaa L., Strömbeck N., Vahtmäe E., 2006, *Monitoring cyanobacterial blooms by satellite remote sensing*, Estuar. Coast. Shelf Sci., 67 (1–2), 303–312, <http://dx.doi.org/10.1016/j.ecss.2005.11.024>.
- Kuvaldina N., Lips I., Lips U., Liblik T., 2010, *The influence of a coastal upwelling event on chlorophyll a and nutrient dynamics in the surface layer of the Gulf of Finland, Baltic Sea*, Hydrobiologia, 639 (1), 221–230, <http://dx.doi.org/10.1007/s10750-009-0022-4>.
- Laanemets J., Väli G., Zhurbas V., Elken J., Lips I., Lips U., 2011, *Simulation of mesoscale structures and nutrient transport during summer upwelling events in the Gulf of Finland in 2006*, Boreal Environ. Res., 16 (suppl. A), 15–26.
- Laanemets J., Zhurbas V., Elken J., Vahtera E., 2009, *Dependence of upwelling-mediated nutrient transport on wind forcing, bottom topography and stratification in the Gulf of Finland: model experiments*, Boreal Environ. Res., 14 (1), 213–225.

- Lass H. U., Mohrholz V., Nausch G., Siegel H., 2010, *On phosphate pumping into the surface layer of the eastern Gotland Basin by upwelling*, J. Marine Syst., 80 (1–2), 71–89, <http://dx.doi.org/10.1016/j.jmarsys.2009.10.002>.
- Lehmann A., Myrberg K., 2008, *Upwelling in the Baltic Sea – A review*, J. Marine Syst., 74 (Suppl.), S3–S12, <http://dx.doi.org/10.1016/j.jmarsys.2008.02.010>.
- Lips I., Lips U., 2008, *Abiotic factors influencing cyanobacterial bloom development in the Gulf of Finland (Baltic Sea)*, Hydrobiologia, 614 (1), 133–140, <http://dx.doi.org/10.1007/s10750-008-9449-2>.
- Lips I., Lips U., 2010, *Phytoplankton dynamics affected by the coastal upwelling events in the Gulf of Finland in July–August 2006*, J. Plankton Res., 32 (9), 1269–1282, <http://dx.doi.org/10.1093/plankt/fbq049>.
- Lips I., Lips U., Liblik T., 2009, *Consequences of coastal upwelling events on physical and chemical patterns in the central Gulf of Finland (Baltic Sea)*, Cont. Shelf Res., 29 (15), 1836–1847, <http://dx.doi.org/10.1016/j.csr.2009.06.010>.
- Männik A., Merilain M., 2007, *Verification of different precipitation forecasts during extended winter-season in Estonia*, HIRLAM Newsletter, 52, 65–70.
- Metsamaa L., Kutser T., Strombeck N., 2006, *Recognising cyanobacterial blooms based on their optical signature: a modelling study*, Boreal Environ. Res., 11 (6), 493–506.
- Myrberg K., Andrejev O., 2003, *Main upwelling regions in the Baltic Sea – a statistical analysis based on three-dimensional modelling*, Boreal Environ. Res., 8 (2), 97–112.
- Myrberg K., Lehmann A., Raudsepp U., Szymelfenig M., Lips I., Lips U., Matciak M., Kowalewski M., Krężel A., Burska D., Szymanek L., Ameryk A., Bielecka L., Bradtke K., Gałkowska A., Gromisz S., Jędrasik J., Kaluźny M., Kozłowski L., Krajewska-Sołtys A., Oldakowski B., Ostrowski M., Zalewski M., Andrejev O., Suomi I., Zhurbas V., Kauppinen O.-K., Soosaar E., Laanemets J., Uiboupin R., Talpsepp L., Golenko M., Golenko N., Vahtera E., 2008, *Upwelling events, coastal offshore exchange, links to biogeochemical processes – Highlights from the Baltic Sea Science Congress at Rostock University, Germany, 19–22 March 2007*, Oceanologia, 50 (1), 95–113.
- Pavelson J., Kononen K., Laanemets J., 1999, *Chlorophyll distribution patchiness caused by hydrodynamical processes: a case study in the Baltic Sea*, ICES J. Mar. Sci., 56 (Suppl.), 87–99, <http://dx.doi.org/10.1006/jmsc.1999.0610>.
- Petersen W., Wehde H., Krasernann H., Colijn F., Schroeder F., 2008, *FerryBox and MERIS – Assessment of coastal and shelf sea ecosystems by combining in situ and remotely sensed data*, Estuar. Coast. Shelf Sci., 77 (2), 296–307, <http://dx.doi.org/10.1016/j.ecss.2007.09.023>.
- Rantajärvi E., Olsonen R., Hallfors S., Leppanen J. M., Raateoja M., 1998, *Effect of sampling frequency on detection of natural variability in phytoplankton: unattended high-frequency measurements on board ferries in the Baltic Sea*, ICES J. Mar. Sci., 55 (4), 697–704, <http://dx.doi.org/10.1006/jmsc.1998.0384>.

- Reinart A., Kutser T., 2006, *Comparison of different satellite sensors in detecting cyanobacterial bloom events in the Baltic Sea*, Remote Sens. Environ., 102 (1–2), 74–85.
- Schroeder T., Behnert I., Schaale M., Fischer J., Doerffer R., 2007a, *Atmospheric correction algorithm for MERIS above Case-2 waters*, Int. J. Remote Sens., 28 (7), 1469–1486, <http://dx.doi.org/10.1080/01431160600962574>.
- Schroeder T., Schaale M., Fischer J., 2007b, *Retrieval of atmospheric and oceanic properties from MERIS measurements: A new Case-2 water processor for BEAM*, Int. J. Remote Sens., 28 (24), 5627–5632, <http://dx.doi.org/10.1080/01431160701601774>.
- Seifert T., Tauber F., Kayser B., 2001, *A high resolution spherical grid topography of the Baltic Sea – 2nd edition*, Baltic Sea Science Congress, Stockholm 25–29 November 2001, Poster No. 147, [<http://www.io-warnemuende.de/iowtopo>].
- Siegel H., Gerth M., Rudolf R., Tschersich G., 1994, *Dynamic features in the western Baltic Sea investigated using NOAA-AVHRR data*, Dt. Hydrogr. Zet., 46, 191–209, <http://dx.doi.org/10.1007/BF02226949>.
- Siegel H., Gerth M., Tschersich G., 2006, *Sea surface temperature development of the Baltic Sea in the period 1990–2004*, Oceanologia, 48 (S), 119–131.
- Sorensen K., Aas E., Hokedal J., 2007, *Validation of MERIS water products and bio-optical relationships in the Skagerrak*, Int. J. Remote Sens., 28 (3–4), 555–568, <http://dx.doi.org/10.1080/01431160600815566>.
- Suikkanen S., Laamanen M., Huttunen M., 2007, *Long-term changes in summer phytoplankton communities of the open northern Baltic Sea*, Estuar. Coast. Shelf Sci., 71 (3–4), 580–592, <http://dx.doi.org/10.1016/j.ecss.2006.09.\break004>.
- Suursaar Ü., Aps R., 2007, *Spatio-temporal variations in hydrophysical and chemical parameters during a major upwelling event off the southern coast of the Gulf of Finland in summer 2006*, Oceanologia, 49 (2), 209–229.
- Uiboupin R., Laanemets J., 2009, *Upwelling characteristics derived from satellite sea surface temperature data in the Gulf of Finland, Baltic Sea*, Boreal Environ. Res., 14 (2), 297–304.
- Vahtera E., Laanemets J., Pavelson J., Huttunen M., Kononen K., 2005, *Effect of upwelling on the pelagic environment and bloom-forming cyanobacteria in the western Gulf of Finland. Baltic Sea*, J. Marine Syst., 58 (1–2), 67–82, <http://dx.doi.org/10.1016/j.jmarsys.2005.07.001>.
- Wu C., 2004, *Normalized spectral mixture analysis for monitoring urban composition using ETM plus imagery*, Remote Sens. Environ., 93 (4), 480–492, <http://dx.doi.org/10.1016/j.rse.2004.08.003>.
- Zhurbas V. M., Laanemets J., Vahtera E., 2008, *Modeling of the mesoscale structure of coupled upwelling/downwelling events and the related input of nutrients to the upper mixed layer in the Gulf of Finland, Baltic Sea*, J. Geophys. Res., 113 (C5), C05004, <http://dx.doi.org/10.1029/2007JC004280>.

Zhurbas V., Oh I. S., Park T., 2006, *Formation and decay of a longshore baroclinic jet associated with transient coastal upwelling and downwelling: A numerical study with applications to the Baltic Sea*, J. Geophys. Res., 111 (C4), C04014, <http://dx.doi.org/10.1029/2005JC003079>.